PHYSICAL REVIEW B **77**, 125323 (2008)

Control of spin coherence in semiconductor double quantum dots

Y. Y. Wang and M. W. Wu*

Hefei National Laboratory for Physical Sciences at Microscale and Department of Physics, University of Science and Technology of China, Hefei, Anhui 230026, People's Republic of China

(Received 18 October 2007; revised manuscript received 18 February 2008; published 18 March 2008)

We propose a scheme to manipulate the spin coherence in vertically coupled GaAs double quantum dots. Up to 10 orders of magnitude variation of the spin relaxation and 2 orders of magnitude variation of the spin dephasing can be achieved by a small gate voltage vertically applied on the double dot. Specially, large variation of spin relaxation still exists at 0 K. In the calculation, the equation-of-motion approach is applied to obtain the electron decoherence time and all the relevant spin decoherence mechanisms, such as the spin-orbit coupling together with the electron-bulk-phonon scattering, the direct spin-phonon coupling due to the phonon-induced strain, the hyperfine interaction, and the second-order process of electron-phonon scattering combined with the hyperfine interaction, are included. The condition to obtain the large variations of spin coherence is also addressed.

DOI: 10.1103/PhysRevB.77.125323 PACS number(s): 72.25.Rb, 73.21.La, 71.70.Ej

I. INTRODUCTION

The fast development of spintronics aims at making devices based on the electron spin. Semiconductor quantum dots (QDs) are one of the promising candidates for the implementation of quantum computations[1–4] because of the relative long spin coherence time, which has been both theoretically[5,6] and experimentally[7–9] proven. Among different kinds of QDs, double quantum dot (DQD) system attracted much more attention recently as there is an additional coupling between two QDs in both vertical[10–12] and parallel[9,13–15] DQDs, which can be conveniently controlled by a small gate voltage. Therefore, spin devices based on DQDs can be designed with more flexibility. So far, many elements of the spintronic devices, such as quantum logical gates,[16,17] spin filters,[18,19] and spin pumps,[18] were proposed and/or demonstrated based on DQD system. Specially, in our previous work, a way to control spin relaxation time (T_1) induced by the spin-orbit coupling (SOC) together with the electron-bulk-phonon (BP) scattering in DQDs by a small gate voltage was proposed.[20] However, according to our latest study,[5] the spin relaxation can be controlled by other mechanisms also, if correctly calculated. In the present paper, we include all the spin decoherence mechanisms following our latest study in the single QD system and apply the equation-of-motion approach to study the spin decoherence in DQD system. By this approach, not only the spin relaxation time but also the spin dephasing time (T_2) can be obtained. We show that both the spin relaxation and the spin dephasing can be manipulated by a small gate voltage in DQD system. Especially, the large variation of spin relaxation still exists even at 0 K. Here, the DQD system studied can be easily realized using the present available technology.

We organize the paper as following. In Sec. II, we set up the model and briefly introduce different spin decoherence mechanisms. The equation-of-motion approach is also simply explained. Then, in Sec. III, we present our numerical results. We first show how the eigenenergies and eigen-wave-functions vary with the bias field in Sec. III A. Then, the electric field dependences of spin relaxation and spin dephasing are shown in Secs. III B and III C, respectively. We conclude in Sec. IV.

II. MODEL AND METHOD

We consider a single electron spin in two vertically coupled QDs with a bias voltage V_d and an external magnetic field $\mathbf{B}$ applied along the growth direction (z axis). Each QD is confined by a parabolic potential $V_c(\mathbf{r})=\frac{1}{2}m^*\omega_0^2\mathbf{r}^2$ (therefore, the effective dot diameter $d_0=\sqrt{\hbar\pi/m^*\omega_0}$) in the x-y plane in a quantum well of width d. The confining potential $V_z(z)$ along the z direction reads

$$V_z(z)=\begin{cases} eEz+\frac{1}{2}eV_d, & \frac{1}{2}a<|z|<\frac{1}{2}a+d \\ eEz+\frac{1}{2}eV_d+V_0, & |z|\leq\frac{1}{2}a \\ \infty & \text{otherwise,} \end{cases} \quad (1)$$

in which V_0 represents the barrier height between the two dots, a stands for the interdot distance, and $E=V_d/(a+2d)$ denotes the electric field due to the bias voltage V_d. Then, the electron Hamiltonian reads $H_e=\mathbf{P}^2/(2m^*)+V_c(\mathbf{r})+V_z(z)+H_Z+H_{SO}$, where m^* is the electron effective mass and $\mathbf{P}=-i\hbar\nabla+\frac{e}{c}\mathbf{A}$ with $\mathbf{A}=(B/2)(-y,x,0)$ being the vector potential. $H_Z=\frac{1}{2}g\mu_B B\sigma_z$ is the Zeeman energy with g, μ_B, and $\boldsymbol{\sigma}$ being the g factor of electron, the Bohr magneton, and the Pauli matrix, respectively. H_{SO} is the Hamiltonian of the SOC. In GaAs, when the quantum well width and the gate voltage along the growth direction are small, the Rashba SOC[21] is unimportant.[22] Therefore, only the Dresselhaus term[23] contributes to H_{SO}. When the quantum well width is smaller than the QD diameter, the dominant term in the Dresselhaus SOC reads $H_{SO}=\frac{1}{\hbar}\Sigma_\lambda\gamma_\lambda^*(-P_x\sigma_x+P_y\sigma_y)$, with $\gamma_\lambda^*=\gamma_0\langle P_z^2\rangle/\hbar^2$. γ_0 denotes the Dresselhaus coefficient, λ is the quantum number of z direction, and $\langle P_z^2\rangle_\lambda\equiv-\hbar^2\int\psi_{z,\lambda}^*(z)\partial^2/\partial z^2\psi_{z,\lambda}(z)dz$, where $\psi_{z,\lambda}$ ($\lambda=1,2,3,\cdots$) is the eigen-wave-function of the electron along the z direction.[20] The electron eigenenergy and wave function in the x-y plane can be obtained by the exact diagonalization approach.[24]

 ©2008 The American Physical Society

The interactions between the electron and the lattice lead to the electron spin decoherence. These interactions contain two parts: one is the hyperfine interaction between the electron and the nuclei and the other is the electron-phonon interaction which is further composed of the electron-BP interaction H_{ep}, the direct spin-phonon coupling due to the phonon-induced strain H_{strain}, and the phonon-induced g-factor fluctuation. We briefly summarize these spin decoherence mechanisms, and the detailed expressions can be found in Ref. 5. (i) The SOC together with the electron-BP scattering H_{ep}. As the SOC mixes different spins, the electron-BP can induce spin relaxation and spin dephasing. (ii) Direct spin-phonon coupling due to the phonon-induced stain H_{strain}.[25] Because this mechanism mixes different spins and also is related to the electron-phonon interaction, it can induce spin decoherence *alone*. (iii) The hyperfine interaction H_{eI}.[26] It is noted that the hyperfine interaction alone only induces T_2 since it only changes the electron spin, but not the electron energy. (iv) The second-order process of hyperfine interaction combined with the electron-BP interaction $V^{(3)}_{eI\text{-}ph}=|\ell_2\rangle[\sum_{m\neq\ell_1}(\langle\ell_2|H_{ep}|m\rangle\langle m|H_{eI}(\mathbf{r})|\ell_1\rangle)/(\varepsilon_{\ell_1}-\varepsilon_m)+\sum_{m\neq\ell_2}(\langle\ell_2|H_{eI}(\mathbf{r})|m\rangle\langle m|H_{ep}|\ell_1\rangle)/(\varepsilon_{\ell_2}-\varepsilon_m)]\langle\ell_1|$, where $|\ell_i\rangle$ $(i=1,2,3,\cdots)$ and ε_{ℓ_i} are the eigenstate and eigenenergy of H_e, respectively. Although the hyperfine interaction cannot induce T_1 alone, it is noted that the second-order process, combined with the electron-BP interaction, can induce both T_1 and T_2. The other mechanisms, including the first-order process of hyperfine interaction combined with the electron-BP scattering[27] and the g-factor fluctuation,[28] have been proved to be negligible.[5]

Due to the SOC, all the states are impure spin states with different expectation values of the spin. For finite temperature, the electron is distributed over many states and therefore one has to average over all the involved processes to obtain the total spin relaxation time. The Fermi-golden-rule approach calculates the spin relaxation from the initial state to the final one whose majority spin polarizations are opposite. However, the average method is inadequate when many impure states are included.[5] Also, the Fermi-golden-rule approach cannot be used to calculate the spin dephasing time. Therefore, in this paper, we adopt the equation-of-motion approach for many-level system with the Born approximation developed in Ref. 5. When the spin dephasing induced by the hyperfine interaction is considered, as the slow relaxation of nuclear bath compared to the electron, the kinetics is non-Markovian. Moreover, because of the Born approximation, this equation-of-motion approach can only be applied for strong magnetic field ($\gtrsim$3.5 T).[29] Therefore, the pair-correlation method[30] is further adopted to calculate the hyperfine interaction induced T_2 for small magnetic field. What should be emphasized is that the SOC is always included, no matter which mechanism is considered. It has been shown that its effect to spin decoherence cannot be neglected.[5]

III. NUMERICAL RESULTS

Following the method addressed above, we perform the numerical calculation in a typical vertically coupled GaAs DQD with barrier height V_0=0.4 eV, interdot distance a=10 nm, and well width d=5 nm. The GaAs material parameters and the parameters related to different mechanisms are the same with those in Ref. 5.

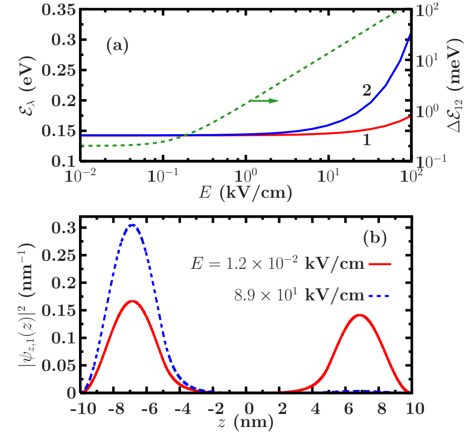

FIG. 1. (Color online) (a) The lowest two eigenenergies along the z-axis $\mathcal{E}_\lambda$ (λ=1,2) and the energy difference $\Delta\mathcal{E}_{12}=\mathcal{E}_2-\mathcal{E}_1$ vs the bias field E. Note the scale of $\Delta\mathcal{E}_{12}$ is on the right side of the figure. (b) Square of the absolute value of the ground state wave function along the z axis at two typical bias fields. In the calculation, the well width d=5 nm, the interdot distance a=10 nm, and the barrier height V_0=0.4 eV.

A. Electric field dependence of eigenenergy and eigen-wave-function along z axis

The eigenenergy and eigen-wave-function along the z direction are numerically obtained. In Fig. 1(a), the lowest two eigenenergies $\mathcal{E}_1$ and $\mathcal{E}_2$ along the z axis and their difference $\Delta\mathcal{E}_{12}=\mathcal{E}_2-\mathcal{E}_1$ are plotted as functions of the electric field E. It can be seen that the energy difference $\Delta\mathcal{E}_{12}$ quickly increases with the electric field E when E is larger than 0.1 kV/cm. The eigen-wave-function of the ground state along the z axis also has large variation with E. It can be clearly seen in Fig. 1(b) that when E is very small (1.2×10^{-2} kV/cm), the wave function of the ground state almost equally locates at the two wells. However, when E is large enough (89 kV/cm), the wave function of the ground state mostly locates at the quantum well with lower potential. The physics of such bias-voltage-induced quick change of eigenenergy and eigen-wave-function can be understood as what follows. Because of the large barrier height V_0 and/or large interdot distance a, the two quantum dots are nearly independent and the eigen-wave-function along the z axis of the lowest subband equally spreads over the two QDs when the source-drain voltage is very small. Therefore, at this time, the energy difference between the lowest two energy levels along the z-axis $\Delta\mathcal{E}_{12}$ is very small. However, with the increase of the source-drain voltage, electron can tunnel through the barrier and the wave function is almost located at one dot with lower potential, and therefore $\Delta\mathcal{E}_{12}$ quickly increases with E.

B. Spin relaxation time T_1 vs electric field E

The spin relaxations due to various mechanisms at different magnetic fields B and quantum dot diameters d_0 are plot-

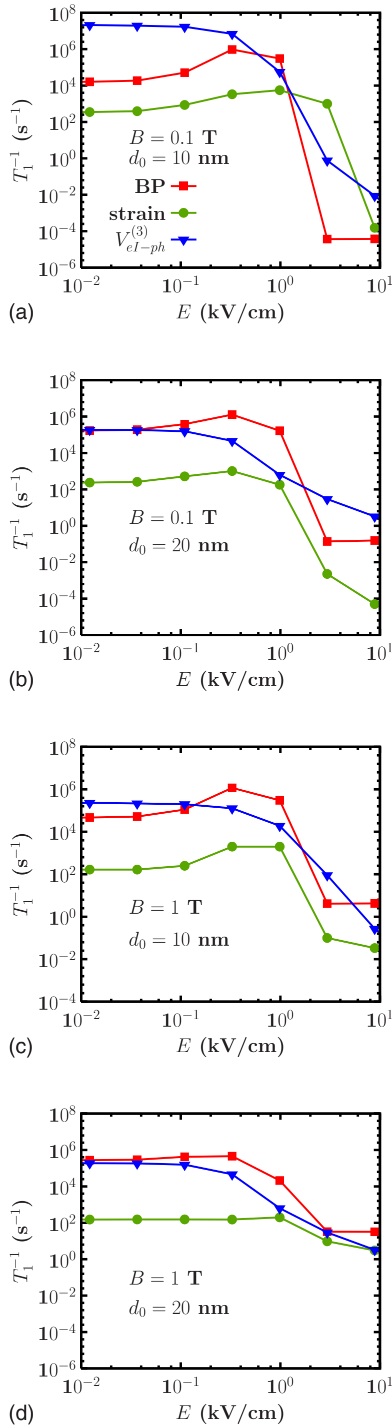

FIG. 2. (Color online) T_1^{-1} induced by different mechanisms vs the electric field at different magnetic fields and dot diameters. T=4 K. Curves with ■: by SOC together with the electron-BP scattering; curves with ●: by the direct spin-phonon coupling due to the phonon-induced strain; curves with ▼: by the second-order process of the hyperfine interaction together with the BP ($V^{(3)}_{eI\text{-}ph}$).

ted as functions of electric field E in Fig. 2. The temperature T=4 K. It is seen that with the increase of E, the spin relaxations induced by all the three mechanisms almost keep unchanged for small E (when $E<0.1$ kV/cm), then increase a little and reach maxima around 0.3 kV/cm. What is interesting is that when E is increased to around 1.1 kV/cm, the spin relaxations are very quickly suppressed over a small window of E. Therefore, the total spin relaxation can be effectively controlled with a small value of the variation of the bias field ΔE. For example, in Fig. 2(a), the spin relaxation shows 10 orders of magnitude variation when the electric field E changes from 0.1 to 10 kV/cm. This can be understood as following. All the three mechanisms are related to the electron-BP scattering which is sensitively affected by the phonon wave length. The scattering becomes most efficient when the phonon wave length is comparable with the dot size. It is also known that the spin relaxations between the first and second subbands are dominant for small electric field.[20] Therefore, when $E<0.1$ kV/cm, as the energy difference between the lowest two subbands along the z-direction $\Delta\mathcal{E}_{12}$ is almost constant [see Fig. 1(a)], the spin relaxation nearly keeps unchanged. When the phonon wave length is comparable with the dot size, the electron-phonon scattering becomes most efficient. Therefore, the spin relaxations show maxima. However, with the further increase of energy difference $\Delta\mathcal{E}_{12}$ by the bias voltage, the phonon wave length becomes larger than the dot size. Consequently, the spin relaxation very quickly decreases over a small window of ΔE.

Now, we focus on the variation magnitude of the spin relaxation with the bias field under different conditions. The largest variation of T_1 (10 orders of magnitude) happens at small magnetic field B=0.1 T and small diameter d_0=10 nm. However, for larger d_0 [20 nm in Fig. 2(b)] or larger B [1 T in Fig. 2(c)], the variations of the total spin relaxation decrease by several orders of magnitude. It is further seen that when both d_0 and B are increased [d_0=20 nm and B=1 T in Fig. 2(d)], the variations of the total spin relaxation are even smaller. This is because the spin relaxation induced by the electron-BP interaction and $V^{(3)}_{eI\text{-}ph}$ decreases with B and d_0 in the high electric field region, where electron is mostly confined in one dot. This is similar to the single QD case.[5] Therefore, to achieve large control of spin decoherence, the magnetic field B and dot diameter d_0 should be small.

We further investigate the electric field dependence of spin relaxation at T=0 K, and the results are shown in Fig. 3. It is interesting to see that the spin relaxation induced by the second-order process of hyperfine interaction combined with the electron-BP scattering ($V^{(3)}_{eI\text{-}ph}$) still has large variation with E (5 orders of magnitude variation when E changes from 0.1 to 10 kV/cm). However, the spin relaxations induced by the other two mechanisms keep almost unchanged. This is because when T=0 K, the electron only locates at the lowest orbital level and the spin relaxation happens only between the lowest two Zeeman sublevels, which keeps unchanged with E. Therefore, the large variations of spin relaxations induced by the SOC together with the electron-BP scattering and the strain-induced direct spin-phonon coupling no longer exist. However, for $V^{(3)}_{eI\text{-}ph}$, which is the second-order process scattering, the middle states $|m\rangle$ can be higher levels as the hyperfine interaction can couple the spin-opposite states in different subbands along the z axis. The energy differences between the middle states and the initial

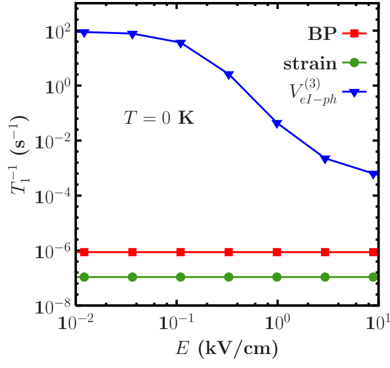

FIG. 3. (Color online) T_1^{-1} induced by different mechanisms vs the electric field. In the calculation, d_0=10 nm, B=0.1 T, and T=0 K. Curve with ■: by SOC together with the electron-BP scattering; curve with ●: by the direct spin-phonon coupling due to the phonon-induced strain; curve with ▼: by the second-order process of the hyperfine interaction together with the BP ($V^{(3)}_{eI\text{-}ph}$).

and/or final states increase with E, and therefore the spin relaxation induced by $V^{(3)}_{eI\text{-}ph}$ quickly decreases with E.

C. Spin dephasing time T_2 vs electric field E

Now, we turn to study the variation of spin dephasing with the electric field E, and the results under different conditions are summarized in Fig. 4. It is seen that the spin dephasing induced by the SOC together with the electron-BP scattering, direct spin-phonon coupling due to the phonon-induced strain, and the second-order process of electron-BP scattering combined with the hyperfine interaction always has several orders of magnitude variation with E at different d_0 and B. However, the spin dephasing induced by the hyperfine interaction only increases a little with E, which suppresses the large variation of the spin dephasing induced by the other three mechanisms. Nevertheless, there is still 2 orders of magnitude variation of the spin dephasing when B and d_0 are small [Fig. 4(a)]. The large variation of spin dephasing induced by the three mechanisms related to electron-phonon scattering comes from the fast increase of the energy difference $\Delta\mathcal{E}_{12}$, similar to the analysis of spin relaxation. The spin dephasing induced by the hyperfine interaction is not so sensitive with E. This is because for the hyperfine interaction, $T_2 \approx E_z A^{-2} N$, which is obtained from the pair-correlation approach, with E_z, A, and N being the Zeeman splitting energy, the hyperfine interaction parameter, and the nuclear number in the quantum dot, respectively.[30] With the increase of the electric field E, E_z and A keep unchanged and the wave function of the ground state is gradually localized on one dot with lower potential. This means that the effective quantum dot size decreases and, consequently, N decreases. However, as the effective quantum dot size decreases from two dots into one dot with the bias field E, N is decreased by only about 50%. Therefore, T_2^{-1} for large field is about two times of that for small field due to the decrease of N. However, this increase of T_2^{-1} induced by the hyperfine interaction is very small compared to that induced by other three mechanisms (which give several orders of magnitude variation). What should be pointed out is that the variation of spin dephasing does not exist at T=0 K. This is because the hyperfine interaction is dominant for the spin dephasing at T=0 K, which keeps unchanged with E.

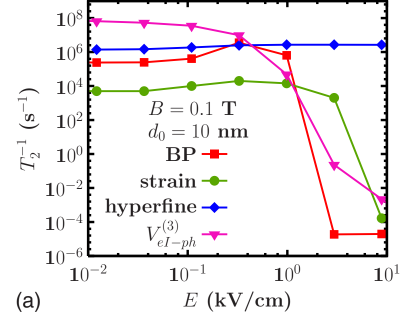

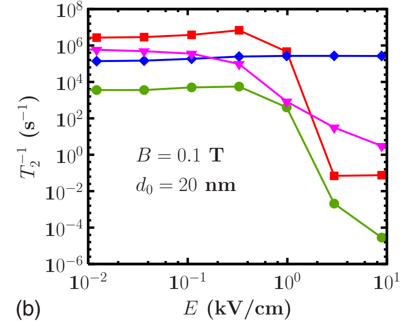

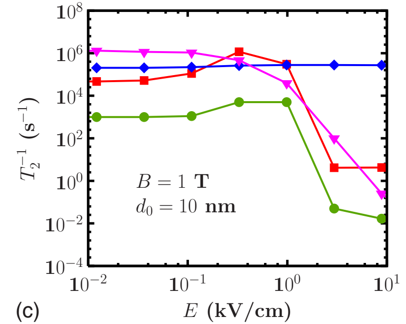

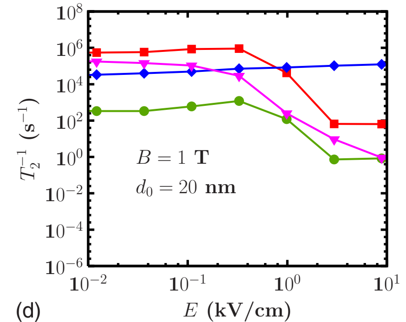

FIG. 4. (Color online) T_1^{-1} and T_2^{-1} induced by different mechanisms vs the electric field at different magnetic fields and dot diameters. T=4 K. Curves with ■: by SOC together with the electron-BP scattering; curves with ●: by the direct spin-phonon coupling due to the phonon-induced strain; curves with ▼: by the second-order process of the hyperfine interaction together with the BP ($V^{(3)}_{eI\text{-}ph}$); curves with ◆: by the hyperfine interaction.

IV. CONCLUSION

In conclusion, we propose a scheme to manipulate the spin decoherence (both T_1 and T_2) in DQD system by a small gate voltage. Up to 10 orders of magnitude of spin relaxation and up to 2 orders of magnitude of spin dephasing can be obtained. To obtain large variation of spin decoherence, the interdot distance and/or the barrier height should be large enough in order to guarantee that the two QDs are nearly independent for the small bias voltage. At the same time, the effective diameter and magnetic field should be small to get as large variation as possible. Finally, based on the present available experimental technology, in this paper, the DQD system applied can be easily realized.[11,12]

ACKNOWLEDGMENTS

This work was supported by the Natural Science Foundation of China under Grants No. 10574120 and No. 10725417, the National Basic Research Program of China under Grant No. 2006CB922005, and the Innovation Project of Chinese Academy of Sciences.

*Corresponding author. mwwu@ustc.edu.cn

[1] *Semiconductor Spintronics and Quantum Computation*, edited by D. D. Awschalom, D. Loss, and N. Samarth (Springer-Verlag, Berlin, 2002); I. Zutic, J. Fabian, and S. Das Sarma, Rev. Mod. Phys. **76**, 323 (2004); R. Hanson, L. P. Kouwenhoven, J. R. Petta, S. Tarucha, and L. M. K. Vandersypen, *ibid.* **79**, 1217 (2007); J. Fabian, A. Matos-Abiague, C. Ertler, P. Stano, and I. Zutić, Acta Phys. Slov. **57**, 565 (2007).

[2] H.-A. Engel, L. P. Kouwenhoven, D. Loss, and C. M. Marcus, Quantum Inf. Process. **3**, 115 (2004); D. Heiss, M. Kroutvar, J. J. Finley, and G. Abstreiter, Solid State Commun. **135**, 591 (2005), and references therein.

[3] D. Loss and D. P. DiVincenzo, Phys. Rev. A **57**, 120 (1998).

[4] J. M. Taylor, H.-A. Engel, W. Dür, A. Yacoby, C. M. Marcus, P. Zoller, and M. D. Lukin, Nat. Phys. **1**, 177 (2005).

[5] J. H. Jiang, Y. Y. Wang, and M. W. Wu, Phys. Rev. B **77**, 035323 (2008).

[6] Y. G. Semenov and K. W. Kim, Phys. Rev. B **75**, 195342 (2007).

[7] R. Hanson, B. Witkamp, L. M. K. Vandersypen, L. H. Willems van Beveren, J. M. Elzerman, and L. P. Kouwenhoven, Phys. Rev. Lett. **91**, 196802 (2003).

[8] S. Amasha, K. MacLean, I. Radu, D. M. Zumbühl, M. A. Kastner, M. P. Hanson, and A. C. Gossard, arXiv:cond-mat/0607110 (unpublished).

[9] J. R. Petta, A. C. Johnson, J. M. Taylor, E. A. Laird, A. Yacoby, M. D. Lukin, C. M. Marcus, M. P. Hanson, and A. C. Gossard, Science **309**, 2180 (2005).

[10] M. Pi, A. Emperador, M. Barranco, F. Garcias, K. Muraki, S. Tarucha, and D. G. Austing, Phys. Rev. Lett. **87**, 066801 (2001).

[11] K. Ono, D. G. Austing, Y. Tokura, and S. Tarucha, Science **297**, 1313 (2002).

[12] D. G. Austing, S. Sasaki, K. Muraki, K. Ono, S. Tarucha, M. Barranco, A. Emperador, M. Pi, and F. Garcias, Int. J. Quantum Chem. **91**, 498 (2003).

[13] F. H. L. Koppens, J. A. Folk, J. M. Elzeman, R. Hanson, L. H. Willems van Beveren, I. T. Vink, H. P. Tranitz, W. Wegscheider, L. P. Kouwenhoven, and L. M. K. Vandersypen, Science **309**, 1346 (2005).

[14] E. A. Laird, J. R. Petta, A. C. Johnson, C. M. Marcus, A. Yacoby, M. P. Hanson, and A. C. Gossard, Phys. Rev. Lett. **97**, 056801 (2006).

[15] P. Stano and J. Fabian, Phys. Rev. B **74**, 045320 (2006); **77**, 045310 (2008).

[16] N. Mason, M. J. Biercuk, and C. M. Marcus, Science **303**, 655 (2004).

[17] R. Hanson and G. Burkard, Phys. Rev. Lett. **98**, 050502 (2007).

[18] E. Cota, R. Aguado, and G. Platero, Phys. Rev. Lett. **94**, 107202 (2005).

[19] F. Mireles, F. Rojas, E. Cola, and S. E. Ulloa, J. Supercond. **18**, 233 (2005).

[20] Y. Y. Wang and M. W. Wu, Phys. Rev. B **74**, 165312 (2006).

[21] Y. Bychkov and E. I. Rashba, J. Phys. C **17**, 6039 (1984).

[22] W. H. Lau and M. E. Flatté, Phys. Rev. B **72**, 161311(R) (2005).

[23] G. Dresselhaus, Phys. Rev. **100**, 580 (1955).

[24] J. L. Cheng, M. W. Wu, and C. Lü, Phys. Rev. B **69**, 115318 (2004); C. Lü, J. L. Cheng, and M. W. Wu, *ibid.* **71**, 075308 (2005).

[25] M. I. D'yakonov and V. I. Perel', Zh. Eksp. Teor. Fiz. **60**, 1954 (1971); [Sov. Phys. JETP **33**, 1053 (1971)].

[26] A. Abragam, *The Principles of Nuclear Magnetism* (Oxford University Press, Oxford, 1961), Chaps. VI and IX.

[27] V. A. Abalmassov and F. Marquardt, Phys. Rev. B **70**, 075313 (2004).

[28] L. M. Roth, Phys. Rev. **118**, 1534 (1960).

[29] W. A. Coish and D. Loss, Phys. Rev. B **70**, 195340 (2004).

[30] W. Yao, R.-B. Liu, and L. J. Sham, Phys. Rev. B **74**, 195301 (2006).